ISROMAC-11 Proceedings of the International Symposium on
Transport Phenomena and Dynamics of Rotating Machinery,
Feb.26-March 2, 2006, Honolulu, Hawaii, USA

Flow around Helicopter Blade Tip Sections Using a 2d Particle Image Velocimeter - Part I

Harika S. Kahveci[1] **& Cengiz Camci**[2]
Turbomachinery Aero-Heat Transfer Laboratory
The Pennsylvania State University
223 Hammond Building, University Park, PA 16802
814 865 9871 fax : 814 865 7092

ABSTRACT

The current study is an effort to better understand the viscous flow physics existing near helicopter blade tips at various angle of attack positions. A planar particle image velocimeter (PIV) was successfully integrated into the helicopter blade tip flow measurement system in a model hover stand The current study utilizes a 1200 mm (47.24 in) diameter scaled helicopter rotor blade system with a 'collective pitch control' capability for flow field measurements. Downwash and upwash behavior at the sections on the blade, and re-circulatory flow behavior near near the tip section are investigated. The specific issues related to the PIV technique used are discussed.

The flow characteristics for 5º pitch case looks like a mirror image of the characteristics for -5º pitch case since the airfoil shape is very close to a symmetrical airfoil. The flow field is found to be relatively symmetric on upper and lower surfaces of the blade when pitch is 0º. Lift is produced at positive pitch case, which leads to a downwash motion in the region by the trailing edge. Similar flow characteristics are observed for negative and positive pitches at different sections away form the tip, but the upwash motion of the flow is more dominant for negative pitch.

INTRODUCTION

This study investigates a helicopter rotor-induced flow field in order to understand the fundamental physics of the rotor near tip flow. The wake that forms behind a helicopter blade is a three dimensional, dynamic flow field. This flow field is affected by blade-vortex interactions and blade-blade interactions. These interactions produce large, unsteady, three dimensional rotor airloads. Today, there is a good understanding of general features of rotor wakes; however, the details of the tip vortices still require more advanced studies [1]. Implementation of non-intrusive measurement systems for complex rotating flow fields in rotorcraft systems has a potential to generate high quality flow physics data especially near rotor blade tip sections.

Development of PIV: Conventional techniques, such as Pitot probe and five-hole probe, have been used so far in various fields to measure velocity and pressure. Although these measurements are reliable to a certain degree, it is known that the existence of a probe in the flow field disturbs the flow pattern. In mid 1970's, Laser Doppler Velocimetry (LDV) technique was developed, which performs time and ensemble averaged measurements, and is a point measuring technique. With this technique, two, and even three velocity components of a steady flow field can be measured simultaneously. When both LDV and hot-wire anemometry are considered, it is obvious that much of today's flow investigations base on point measuring techniques.

More recently, Particle Image Velocimetry (PIV) system was developed in order to measure the instantaneous whole-field velocity data. PIV is capable of measuring unsteady flow phenomena within complex flow fields; that is, both steaqdy and transient flows can be studied. Instantaneous velocity field measurements can be performed. Since it is a planar measurement technique, multiple points can be measured at the same time. Both PIV and LDV suffer from near wall effects where a probe volume or laser sheet generates significant reflections from the wall. A related discussion can be found in reference [3], including optical access, light sheet delivery and particulate seeding.

At this point, it will be useful to classify laser techniques as point and planar measurement techniques. For point measurements, a focused laser is used, whereas for planar measurements, a laser sheet is utilized. Besides LDV, another point measurement technique is Phase Doppler Anemometry (PDA), which is an extension of LDV, and

1 Graduate Res. Asst. , presently at GE Power Systems, Greenville, SC
2 Professor of Aerospace Engineering, (cxc11@psu.edu)

gives time averaged pointwise measurements of droplet size and velocity. PDA is known to be a well-established technique for droplet size measurements in spray characterization experiments.

If the particle concentration used for seeding is too dense, the individual particles appear as speckles rather than dots on the image plane. This technique is referred to as Laser Speckle Velocimetry (LSV).

It should be noted that laser based techniques use electromagnetic radiation instead of a physical probe, so that the flow field remains undisturbed. However, the particles in the flow field still have an interaction with the electromagnetic radiation, which is known as scattering. Among the planar measurements, besides PIV, Mie Scattering and Planar Laser Induced Fluorescence (PLIF) techniques are widely used, especially in spray field, since they give information about mass distribution and droplet characteristics. PLIF provides time averaged steady flow measurements, and obtains spatial variations of droplets, as well as their mass distribution.

2D PIV Applications: There have been many studies performed using 2D PIV until the development of 3D PIV. Although 3D PIV has the advantage of calculating the third velocity component as well, its complex test configuration and high cost let 2D PIV be a still widely used technique. The configuration becomes more complex because of the additional camera, and this causes problems when especially used for rotating machinery experiments. As it is the case for all innovations, the 2D PIV has started to be applied first for simple flow fields, such as flow investigation over an airfoil performed by Lourenco et al [4], and expanded its area of use to more complex flows such as in turbomachines, later on.

One of the 2D PIV applications was held by Sanders et al [5] in a transonic compressor in order to investigate the rotor and inlet guide vane (IGV) interactions. In this research, it was observed that due to high speed, the shocks occurring at the rotor leading edge impacted with the vane trailing edge, resulting in a complicated time-dependent wave pattern in the vane passage. They also investigated multi-blade row interactions in an axial-flow compressor, and compared the rotor wakes at subsonic and transonic operating conditions [6]. Wuibaut et al [7] successfully performed flow characterization measurements in the outlet part of a centrifugal pump with this technique. Flow over a simple commercial wind turbine was examined using a 2D PIV technique by Grant et al [8].

As well as turbomachinery, PIV technique was used in different environments such as the exhaust of small solid rocket motors. Balakumar and Adrian performed 2D PIV measurements in the harsh environments such as background irradiance from burning gases, inability to control seeding densities, and compressibility effects [9]. A previous study in this field other than using 2D PIV is analysis of scattering characteristics by Yan et al [10]. Axial flow and secondary flow patterns in a 90-degree bifurcation were explored with 2D PIV by Nikolaidis and Mathioulakis [11] for medical purposes in order to find an answer to why arteriosclerosis develops in branches of human circulatory system.

Flow Around Helicopter Rotor Blades: The flow is unsteady due to blade boundary layers, 3D flow near the tip and vortex shedding especially at high angle of attack. The flexible motion of the rotor blades also makes the secondary flows and tip vortices more difficult to understand compared to flow around the antenna.

During the rotation of the helicopter blades, vortices created at blade tips have a strong effect on the overall rotor flow field. This effect dominates for many rotations, which has a consecutive effect on aerodynamic loading of blades. For a maneuvering helicopter, the rotor performance and dynamics are further affected, and this phenomenon is called 'blade vortex interaction, (BVI)'. This interaction introduces more airloads acting on the blades, and results in an increased noise generation. Therefore, the flow characteristics around helicopter blades need to be investigated to have a better understanding of how the rotor performance, acoustics, and loads are affected during the flight.

There have been many studies performed to investigate the flow characteristics of rotor blades. First studies were carried out by using hot-wires or pressure probes. Wind tunnels have been utilized to measure the rotor blade pressures during flight. Lorber [12] used a pressure-instrumented helicopter model under level, hover, and descent conditions, and obtained several measurements for blade pressures and wake interactions by wind tunnel testing. It was observed that the BVI events were repeatable and consistent.

In order to understand the flow field and noise-generating mechanisms, some computational codes were developed as well. Within an international cooperative program, a helicopter model was tested in the German Dutch Wind Tunnel (DNW), and the data was compared with numerical methods developed by DLR of Germany, ONERA of France, and the Aeroflightdynamics Directorate (AFDD) of the U.S. Army [13]. Blade surface pressures, vortex core size and trajectories were examined. It was concluded that in order to improve the prediction capabilities, more experimental data is needed for detailed wake information.

Limitations of experimental work such as flow disturbance by probes, and unresolved time-dependent nature of the flow were overcome by the introduction of laser techniques in flow field investigations. Leishman et al [1, 14-17] have performed many studies using three-dimensional Laser Doppler Velocimetry technique. In these studies, three-dimensional velocity field, circulation profiles, aperiodicity effects, and turbulence quantities were investigated for single and two-bladed rotors.

Besides LDV studies, 2D PIV has also been applied for rotor analysis so far. Raffel et al [18] measured blade tip vortices by utilizing both LDV and 2D PIV techniques. The both techniques were compared for the first time using the same rotor in a wind tunnel. The recording of the PIV images were performed phase-locked with the rotor motion. It was observed that the results obtained were similar, with the advantage of less time needed by PIV technique.

For rotating flow fields, PIV is found to be more efficient to be used over large areas. A variation of 2D PIV was developed and applied to a flow field generated by a four-bladed helicopter rotor by Saripalli et al [19]. The velocity and vorticity measurements were made and compared with other published data. A Blade-Vortex Interaction (BVI) study with secondary vertical structures investigation was performed over a single-blade rotor disk by Horner et al [20]. A stationary wing was subjected to an oncoming vortex generated upstream of the rotor disk, and the data for different azimuth angles were compared.

PIV DETAILS

PIV technique can be described as a technique used to measure instantaneous velocity components of a flow field over a determined area [21-24]. Small particles are introduced into the flowing medium, and the region of interest is illuminated by the light sheet provided by short laser pulses. The subsequent step is the recording of the displacement of particles via one or two CCD cameras depending on the PIV technique used. As a summary, four basic steps should be mentioned in an experimental procedure:

1. Flow is seeded.
2. The flow region of interest is illuminated.
3. Scattering light from the particles is recorded by cameras.
4. Recordings are analyzed by means of software.

As also explained by R.J. Adrian [25], the scattered light from seeding particles are recorded by a camera (in the case of 3D PIV, two different cameras do the simultaneous recording). The initial position of a particle is recorded on the first frame of the camera right after first laser pulse fires. Its final position is recorded in the same way on the second frame of the same camera when the second laser pulse fires. Since the displacement of the particle and the time interval between laser pulses are known, the velocity of the particle can be calculated by the simple equation: speed=distance/time.

TEST SETUP

An IKARUS ECO 16 model helicopter with a two-bladed rotor is used for the experiments. The model has a main rotor diameter of 1200 mm (47.24 in), and the untwisted blades have a 42 mm (1.65 in) chord length. A 4Z143 Dayton permanent magnet DC motor is used to drive the rotor. The experiments are performed for a 9.5 Hz of frequency which corresponds to 570 rpm, giving a tip velocity of 35.8 m/s (117.5 ft/s) and a tip Reynolds number of 9.6 x 10^4. The experiments are carried out without any cross-wind or flight velocity.

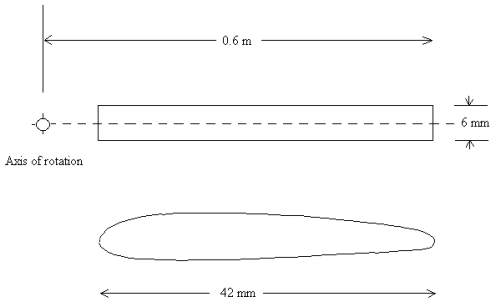

Figure 1. Geometrical characteristics of airfoil

PIV system used in the experiment consists of two laser units, a camera, a fog generator, a processor and software. The New Wave Research Gemini-PIV Nd:YAG laser is used for the illumination purpose. This system consists of two power supplies, two IR laser heads, and a double-cavity Q-switched Nd:YAG laser. For a Nd:YAG laser, the typical amount of pulse energy is 200 mJ (0.0002 btu), and its duration is usually less than 10 ns.

A 80C60 HiSense PIV/PLIF camera with 1024 x 1280 pixels is used with 80N57 Personality Module fitted to processor, and a Nikon Micro-Nikkor 60/2.8 objective.

The instrument Rosco Omega-XT used as the seed generator in the experiments uses a mixture of triethylene glycol, propylene glycol, 1,3 butylene glycol and de-ionized water, which has a particle diameter of 0.25-60 μm (0.0098-0.024 mils).

The synchronization of the pulsating of the light sheet with the recording of the images and data analysis in PIV measurements are all performed by DANTEC PIV 2000 processor unit. This unit controls not only recording, but also illumination. All of the data reduction procedures for the image pairs that are obtained by cameras are done by Flow Manager Software.

The measurements are obtained in two vertical planes cutting the blade, which corresponds to the distances of 5 cm (1.97 in) and 10 cm (3.94 in) away from the tip as shown in Fig. 2. The distances in the figure are exaggerated for clarity. For each location, the blade is given -5º, 0º, and 5º pitch. The experiments are run in phase-locked by

applying some trigger delay to capture the image of the blade at the same location throughout different measurements. The blade position parallel to the bench carrying the two cameras and the laser is always used during the phase locked measurements. The laser sheet thickness is set to be 6 mm (0.24 in).

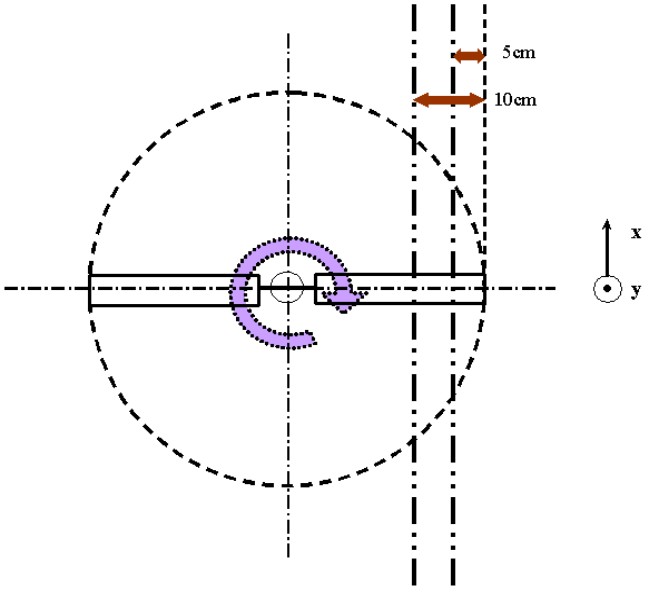

Figure 2. Laser sheet locations on the helicopter blade for 2D analysis

The recordings taken by the camera all need to correspond to the same location of the blades during rotation. An infrared emitter-receiver based once-per-rev (OPR) device is used to trigger the sequence of events. In order the processor to command the lasers to give the shots with a correct timing, the laser mode is made 'asynchronous', and an 'external burst trigger' is applied. In order to have the cross section to be located in the middle of the camera view, a trigger delay is provided. A clean TTL signal produced by the OPR device defines the specific time for PIV data acquisition.

Figure 3 shows an image taken during the experiment where the blade had a -5º pitch and the laser is on the section 5 cm (1.97 in) away from the tip. A large number of vector maps, such as 1200, are collected for statistical analysis of the results for accuracy. 1200 image pairs provide a statistically stable mean flow definition after ensemble averaging.

The rotational direction of the helicopter blade is from right to left in the current experiment. Since the laser sheet generates a shadow in front of the leading edge, back zone

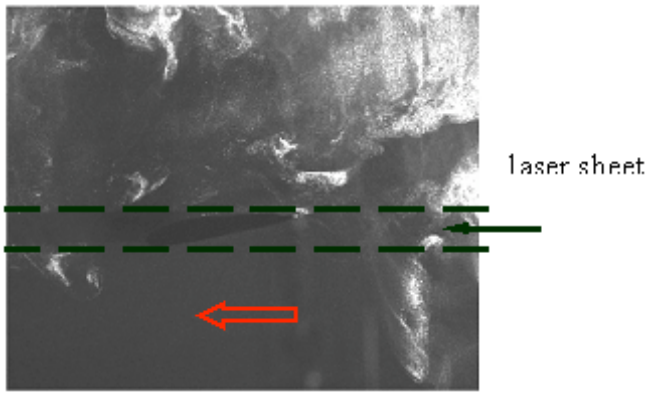

Figure 3. An image of flow field captured during the experiment

with no illumination cannot provide velocity vector measurements. The area between dashed lines is masked before any data processing is applied to raw speckle images. The airfoil section is also masked because of the same reason.

Figure 4 represents the masking applied across the airfoil cross-section and in the region where the shadow occurs. No data can be obtained among the masked area. This can be observed in the vector maps.

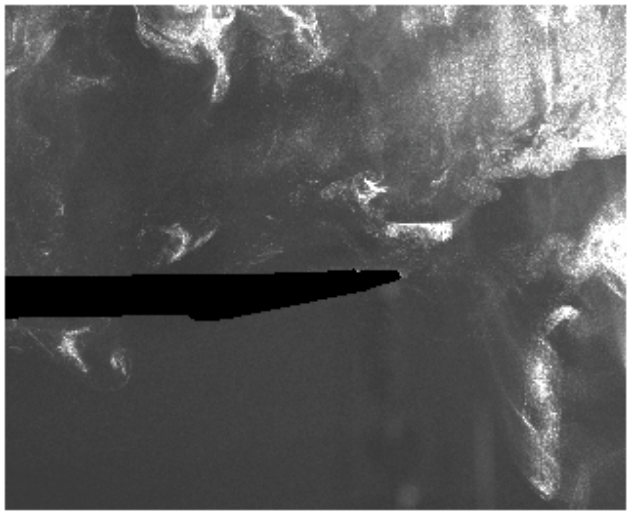

Figure 4. A masked flow field image

For processing, the adaptive-correlation is applied for a 16x16 interrogation area with settings of zero overlap and a peak validation of 1.1.

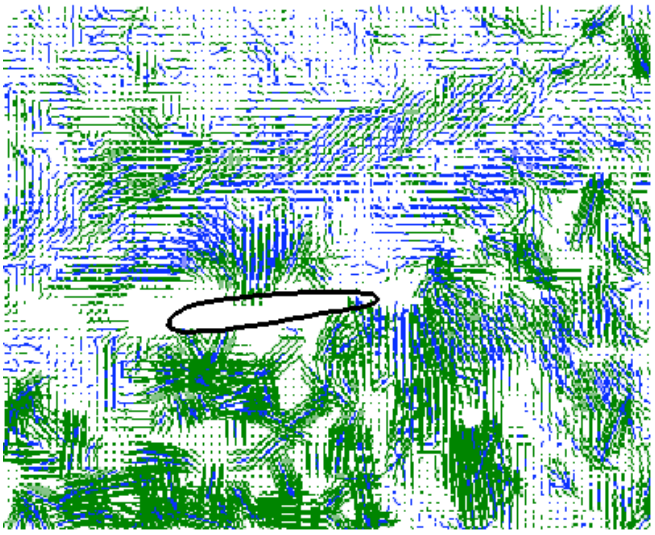

Figure 5. An instantaneous vector map obtained by adaptive-correlation

EXPERIMENTAL RESULTS AND DISCUSSIONS

5 cm (1.97 in) Away From the Tip: The measurement plane is 5 cm away from the tip in radially inward direction.

-5º Pitch: For 2D PIV analysis of all vector maps, every other vector in x-direction, and every 2 vectors out of 3 in y-direction have been omitted. Figure 6 shows the vector map, which belongs to ensemble averaging of 1200 data sets. The velocity magnitude has been demonstrated with colored contours.

The blade is located in the flow field as it is observed from the speckle images given above. There are almost no velocity vectors in the masked regions corresponding to the shadow and the blade itself, as expected. Due to negative pitch, there is an upwash observed in the whole flow field. A vorticity variation in blade boundary layers and in the wake region is apparent. A distributed negative vorticity across the chord on the lower surface is obvious.

The flow is deflected away by the motion of leading edge, moving in different directions. It moves towards trailing edge to fill the space evacuated by the blade. In this region, there is not as much scatter in the direction of the flow as in the front region. The velocity has its highest values near the mid chord location of the upper and lower surfaces in general. The lowest velocity values are near trailing edge of the upper surface. Here, the flow has a tendency to move towards the aft point. The lower surface flow at negative incidence has a curved path connecting the leading edge zone to the trailing edge zone. The strongest

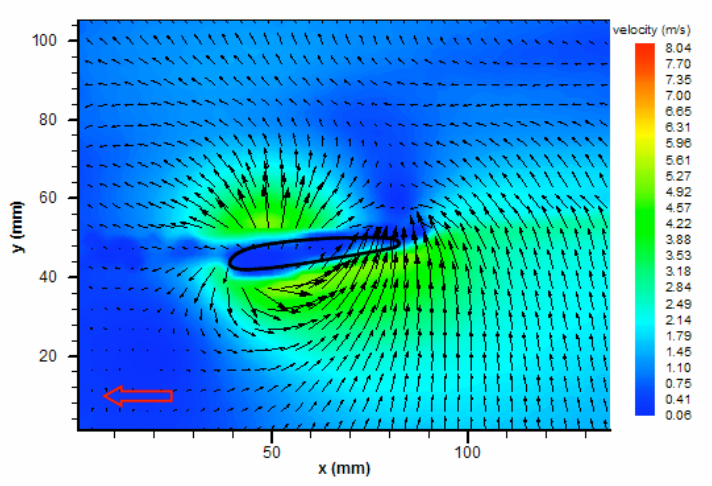

Figure 6. 2D vector map with colored contours at -5º pitch 5 cm (1.97 in) away from the tip

upwash components are near the trailing edge on the lower surface of the blade.

The whole flow field itself appears to be highly re-circulatory, having the flow move towards left on the upper region far from the blade, and the upwash in the right region, ending up in a counterclockwise motion altogether.

0º Pitch: In Fig.7, blade is demonstrated in its corresponding location in the flow field for 0º pitch. Since there is no pitch applied to the blade, the flow field appears to be relatively symmetric on upper and lower surfaces of the blade. Some vorticity distribution across the chord on both surfaces can be observed, although it is not as strong as it is for the case of -5º pitch. The flow is disturbed again by the motion of the blade. It moves away from leading edge in different directions, whereas the motion towards trailing edge is more obvious in this case.

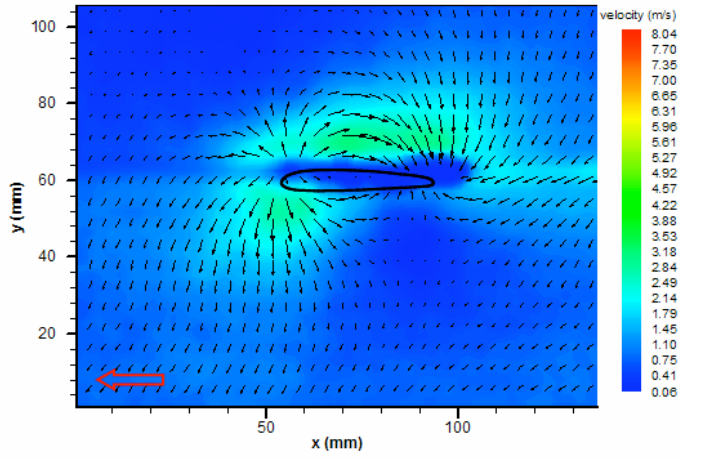

Figure 7. 2D vector map with colored contours at 0º pitch 5 cm (1.97 in) away from the tip

The green velocity vectors in the map occupy a much smaller percentage of the measurement domain when compared to -5º pitch. The leading edge of the airfoil induces upwash components near the top of the airfoil. Downwash components are visible in the lower part of the blade where leading edge curvature is still dominant. The airfoil clearly drags some fluid behind its trailing edge in almost horizontal direction.

5º Pitch: Figure 8 shows that the flow characteristics for 5º pitch case looks like a mirror image of the characteristics for -5º pitch case since the airfoil shape is very close to a symmetrical airfoil.

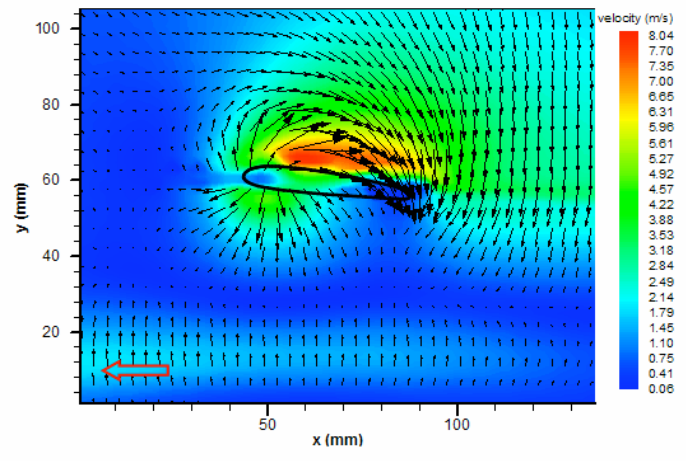

Figure 8. 2D vector map with colored contours at 5º pitch 5 cm (1.97 in) away from the tip

There is an obvious downwash motion in the region by the trailing edge due to the lift produced. The whole flow field can be considered as vorticity in clockwise direction. The difference is that the velocity magnitudes are higher on the upper surface of the blade in a positive pitch. The velocity vectors below Y=30 mm (1.18 in) have a small but upwash component. This upward flow may be due to the part of the flow reflecting from the ground. This is especially a strong effect near the tip. The ground to 'rotor plane' distance is 132 cm (52 in).

10 cm (3.94 in) Away From the Tip: The measurement plane is 10 cm (3.94 in) away from the tip in radially inward direction.

-5º Pitch: As it is in the case of negative pitch at the section 5 cm (1.97 in) away from the tip, similar flow characteristics are observed at this section of 10 cm (3.94 in) away from the tip. The difference is that the velocity magnitudes across the whole flow field are higher than that of 5 cm (1.97 in) section. But, the green high velocity magnitude zone below the airfoil occupies a relatively smaller area when compared to near tip measurements of 5º pitch 5 cm (1.97 in) away from the tip. The upwash motion of the flow is more dominant across the whole region, hence the whole flow field itself can not be considered as a vorticity.

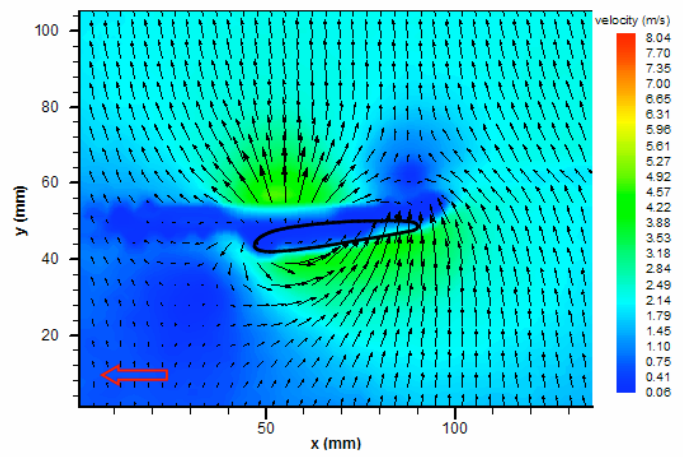

Figure 9. 2D vector map with colored contours at -5º pitch 10 cm (3.94 in) away from the tip

0º Pitch: Similar flow characteristics are observed at this section again, as in the case of 0º pitch at the section 5 cm (1.97 in) away from the tip. But, the magnitude is higher around the blade on upper and lower surfaces; hence the vorticity at 10 cm (3.94 in) section is more significant for 0º pitch as a contradictory to negative pitch case.

The green high velocity magnitude zone is enlarged compared to near tip measurement. This may be due to the fact that tip effects are felt at a much less significant rate at this section.

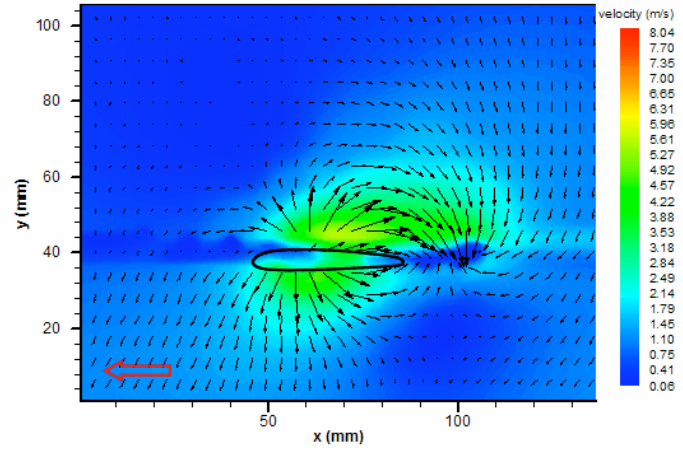

Figure 10. 2D vector map with colored contours at 0º pitch 10 cm (3.94 in) away from the tip

5º Pitch: In the case of positive pitch at the section 10 cm (3.94 in) away from the tip, the flow characteristics are similar to the section near the tip. The velocity magnitude across the whole flow field is higher than that of 5 cm (1.97 in) section, as it is observed for negative pitch case. The velocity magnitudes are reduced on upper surface of the blade. The downwash motion of the flow is more dominant across the whole region, hence the whole flow field itself can not be considered as a vorticity.

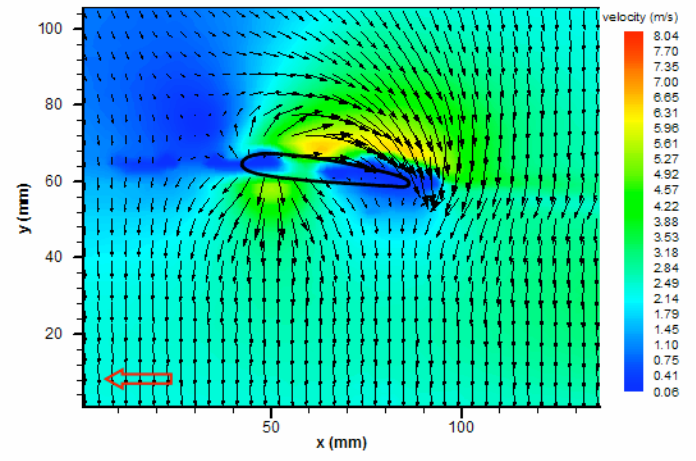

Figure 11. 2D vector map with colored contours at 5º pitch 10 cm (3.94 in) away from the tip

A significant characteristic of this region is the fact that there is no ground effect producing velocity components in a direction from the ground to rotor. Downwash is fully dominant underneath the rotor. The flow below the rotor has slightly more kinetic energy because of the elimination of ground influence. Velocity magnitudes on the top surface are also reduced mainly because of the clean boundary layer formation without a tip vortex generating additional re-circulatory motion.

When Fig. 11 is examined, it can be observed that the flow characteristics for positive pitch case looks like a mirror image of the characteristics for negative pitch case at this section, as well.

CONCLUSIONS

In this research, a 2D PIV technique is utilized successfully and details for the near tip flow field in a helicopter rotor system is captured in a short time. The results are obtained in aphase-locked arrangement for a selected position of the helicoptrer rotor.

A set of measurements from a 1200 mm (47.24 in) diameter scaled helicopter rotor blade system with a 'collective pitch control' capability is analyzed. 2D PIV technique is applied to this system, for a rotor speed of 570 rpm, and -5º, 0º, and 5º pitch. The experiments are run at different radial locations near the tip.

It is observed that ground effect decreases with a higher positive pitch and at a section further away from the tip. Also, away from the tip, vorticity on the airfoil surfaces decreases. Downwash and upwash behavior becomes more significant across this whole region due to a much cleaner boundary layer. The flow characteristics for 5º pitch case looks like a mirror image of the characteristics for -5º pitch case since the airfoil shape is very close to a symmetrical airfoil. The flow field is found to be relatively symmetric on upper and lower surfaces of the blade when pitch is 0º. Lift is produced at positive pitch case, which leads to a downwash motion in the region by the trailing edge. Similar flow characteristics are observed for negative and positive pitches at different sections away form the tip, but the upwash motion of the flow is more dominant for negative pitch.

For each experiment presented in this study, 1200 data sets (double frames) are collected and ensembled to have good results for statistical analysis of turbulence characteristics.

Since an ensemble size of 1200 is used, storage of data creates a problem for the system. A total space of about 200GB was used during the experiments.

Having a speckle image distribution as homogeneous as possible is important, because either insufficient or excessive amount of fog results in more errors in vector calculations. As a solution, fog is provided at every 100-data interval to keep the distribution homogeneous. Isolating the laboratory where the experiments are performed is also recommended.

The laser reflections encountered during the experiments from the surfaces of interest cause some loss of data.Masking is required to be applied to reflection regions in order to avoid the miscalculations in those areas. With masking, it is also possible that some useful data are also handicapped. Therefore, it is necessary to avoid the laser reflections in an effective manner. With this purpose, some fluorescent type paint is used in experiments. Fluorescent paint was not enough to reduce the reflection completely from the surface due to the high intensity of the laser light. Besides the laser light, the environmental lighting and solar influence coming from the windows should also be avoided.

The flow field around rotating machinery components is observed to have significant circulatory type of characteristics. The flow may also be disturbed by some obstacles present in the surroundings, which may deflect it from its three dimensional and complex pattern. In order to obtain reliable results, there should be no objects in the flow field other than the rotating component itself. It is recommended that any unrelated objects present in the experiment area be removed.

REFERENCES

[1] Leishman, J. G., Baker, A., Coyne, A., 1996, "Measurements of Rotor Tip Vortices Using Three-Component Laser Doppler Velocimetry," Journal of the American Helicopter Society, **41**, No.4, pp. 342-353.

[2] Jørgensen, F. E., 2002, "How to Measure Turbulence with Hot-wire Anemometers," Dantec Dynamics.

[3] Wernet, M. P., "PIV for Turbomachinery Applications," National Aeronautics and Space Administration Lewis Research Center, Cleveland, OH, NASA TM-107525

[4] Lourenco, L., Krothapalli, A., Buchlin, J. M., Riethmuller, M. L., 1986, "Noninvasive Experimental Technique for the Measurement of Unsteady Velocity Fields," AIAA Journal, **24**, pp.1715-1717.

[5] Sanders, A.J., Papalia, J., Fleeter, S., 2002, "A PIV Investigation of Rotor-IGV Interactions in a Transonic Compressor," Journal of Propulsion and Power, **18**, No. 5. pp. 969-977.

[6] Sanders, A.J., Papalia, J., Fleeter, S., 2002, "Multi-Blade Row Interactions in a Transonic Axial Compressor: Part I-Stator Particle Image Velocimetry (PIV) Investigation, " Journal of Turbomachinery, **124**.

[7] Wuibaut, G., Dupont, P., Bois, G., Caignaert, G., Stanislas, M., 2001, "Analysis of Flow Velocities Within the Impeller and the Vaneless Diffuser of a Radial Flow Pump," Proc. Instn. Mech. Engrs. **215**, Part A.

[8] Grant, I., Smith, G. H., Liu, A., Infield, D., Eich, T., 1991, "Measurement of Shed Vorticity and Circulation From Rotating Aerofoil by Particle Image Velocimetry, 4th International Conference on Laser Anemometry, Advances and Applications," Cleveland, OH.

[9] Balakumar, B. J., Adrian, R. J., "Particle Image Velocimetry in the Exhaust of Small Solid Rocket Motors, " University of Illinois.

[10] Yan, D., Zhang, J., He, A., Zhang, L., 1993, "Experimental Studies on Laser Scattering From Exhaust Jet of a Real Rocket," Proc. SPIE **2005**, 'Optical Diagnostics in Fluid and Thermal Flow', Ed. Soyong S. Cha and James D. Trolinger, pp.86-93.

[11] Nikolaidis, N. M., Mathioulakis, D. S., 2002, "Axial and Secondary Flow Study in a 90 Deg Bifurcation Under Pulsating Conditions Using PIV," Journals of Fluids Engineering, **124**.

[12] Lorber, P. F., 1990, "Aerodynamic Results of a Pressure-Instrumented Model Rotor Test at the DNW," 46th Annual Forum of American Helicopter Society, Washington D.C.

[13] Yu, Y. H., Tung, C., Gallman, J., Schultz, K. J., Van Der Wall, B., Spiegel, P., Michea, B., 1993, "Aerodynamics and Acoustics of Rotor Blade-Vortex Interactions," AIAA 15th Aeroacoustics Conference, paper 93-4332, Long Beach, CA.

[14] Leishman, J. G., Bhagwat, M. J., 1999, "Correlation of Helicopter Rotor Tip Vortex Measurements," AIAA Journal.

[15] Leishman, J. G., 1998, "Measurements of the Aperiodic Wake of a Hovering Rotor," Experiments in Fluids, **25,** pp. 352-361, Springer-Verlag.

[16] Han, Y. O., Leishman, J. G., Coyne, A. J., 1997, "Measurements of the Velocity and Turbulence Structure of a Rotor Tip Vortex," AIAA Journal, **35**, No. 3.

[17] Coyne, A. J., Bhagwat, M. J., Leishman, J. G., 1997, "Investigation Into the Rollup and Diffusion of Rotor Tip Vortices Using Laser Doppler Velocimetry," American Helicopter Society 53rd Annual Forum, Virginia Beach, VA,.

[18] Raffel, M., Seelhorst, U., Willert, C., 1996, "Vortical Flow Structures at a Helicopter Rotor Model Measured by LDV and PIV," 22nd European Rotorcraft Forum, Brighton, UK.

[19] Saripalli, K. R., 1995, "Application of Particle Imaging Velocimetry Techniques to Helicopter Rotor Flowfields at McDonnell Douglas Aerospace," 33rd AIAA Aerospace Sciences Meeting and Exhibit, Reno.

[20] Horner, M. B., Stewart, J. N., Galbraith, R. A. McD., Grant, I., Coton, F. N., 1994, "An Examination of Vortex Deformation During Blade-Vortex Interaction Utilising Particle Image Velocimetry," 19th Congress of the International Council of the Aeronautical Sciences, **2**.

[21] DANTEC, Particle Image Velocimetry: An Informative Seminar on PIV Techniques for Whole Field Flow Measurements

[22]DANTEC, FlowMap 3D-PIV System-Installation & User's Guide.

[23]DANTEC, 1998, "FlowMap Particle Image Velocimetry Systems - Integrated Real-time PIV Instrumentation,".

[24]DANTEC, 2000, "FlowMap Particle Image Velocimetry Instrumentation-Installation & User's Guide".

[25] Adrian, R. J., 1991, "Particle Imaging Techniques for Experimental Fluid Mechanics," Ann. Rev. Fluid Mech., **23**, pp. 261-304.

5 cm (1.97 in) away from the tip		-5° pitch		0° pitch		5° pitch	
		Calibration	*Laser Setup*	*Calibration*	*Laser Setup*	*Calibration*	*Laser Setup*
Mode		_	Asynchronous	_	Asynchronous	_	Asynchronous
Acquisition Control	*exposure (time between pulses)*	30000 µs	100 µs	30000 µs	100 µs	30000 µs	100 µs
	burst start	user action from PC	external burst trigger	user action from PC	external burst trigger	user action from PC	external burst trigger
	trigger delay	_	3400.20 µs	_	2001.80 µs	_	2630.60 µs
Field of View	*scale factor*	16.108	16.108	16.922	16.108	16.068	16.068
	object width	138.1 mm (5.44 in)	138.1 mm (5.44 in)	145.1 mm (5.71 in)	138.1 mm (5.44 in)	137.8 mm (5.43 in)	137.8 mm (5.43 in)
	object height	110.5 mm (4.35 in)	110.5 mm (4.35 in)	116.1 mm (4.57 in)	110.5 mm (4.35 in)	110.2 mm (4.34 in)	110.2 mm (4.34 in)

Table 1. Calibration and Laser Setup Parameters - I

10 cm (3.94 in) away from the tip		-5° pitch		0° pitch		5° pitch	
		Calibration	*Laser Setup*	*Calibration*	*Laser Setup*	*Calibration*	*Laser Setup*
Mode		_	Asynchronous	_	Asynchronous	_	Asynchronous
Acquisition Control	*exposure (time between pulses)*	30000 µs	100 µs	30000 µs	100 µs	30000 µs	100 µs
	burst start	user action from PC	external burst trigger	user action from PC	external burst trigger	user action from PC	external burst trigger
	trigger delay	_	2800.20 µs	_	2800.20 µs	_	2849.80 µs
Field of View	*scale factor*	16.842	16.842	17.481	17.481	16.975	16.975
	object width	144.4 mm (5.69 in)	144.4 mm (5.69 in)	149.9 mm (5.90 in)	149.9 mm (5.90 in)	145.6 mm (5.73 in)	145.6 mm (5.73 in)
	object height	115.5 mm (4.55 in)	115.5 mm (4.55 in)	119.9 mm (4.72 in)	119.9 mm (4.72 in)	116.5 mm (4.59 in)	116.5 mm (4.59 in)

Table 2. **Calibration and Laser Setup Parameters – II**

"X	"Y	"X	"Y	"X [mm]"	"Y [mm]"	"X [mm]"	"Y [mm]"
3.83	3.43	13.04	5.71	37.71	4.43	24.55	2.19
3.89	3.67	13.96	5.71	38.27	4.34	23.57	2.14
4.01	3.89	14.85	5.73	38.85	4.24	22.07	2.09
4.26	4.12	15.73	5.74	39.31	4.10	20.23	2.04
4.53	4.30	16.96	5.74	39.73	3.92	18.03	1.98
4.81	4.48	18.06	5.74	39.98	3.75	15.86	1.96
5.14	4.65	19.22	5.70	40.16	3.51	14.08	1.95
5.45	4.75	20.36	5.67	40.13	3.26	12.73	1.92
5.79	4.87	21.49	5.65	39.92	3.05	11.57	1.94
6.06	4.95	22.78	5.59	39.52	2.91	10.35	1.97
6.40	5.04	24.24	5.54	39.06	2.81	9.24	2.03
6.73	5.12	25.65	5.48	38.57	2.78	8.08	2.05
7.04	5.19	27.12	5.38	38.02	2.74	7.07	2.12
7.38	5.26	28.44	5.29	37.47	2.71	6.06	2.26
7.74	5.33	29.72	5.20	36.64	2.68	5.51	2.38
8.14	5.40	31.07	5.08	35.76	2.63	5.02	2.50
8.60	5.46	32.36	4.95	34.74	2.58	4.62	2.64
9.18	5.51	33.43	4.90	33.70	2.53	4.29	2.79
9.86	5.57	34.44	4.81	32.42	2.50	4.04	2.98
10.62	5.62	35.42	4.73	30.55	2.42	3.87	3.14
11.36	5.67	36.24	4.64	28.38	2.33	3.80	3.26
12.21	5.70	37.07	4.53	26.27	2.25	3.81	3.35

Table 3. Airfoil Coordinates